ELSEVIER

Journal of Organometallic Chemistry 504 (1995) 75–91

Journal of Organometallic Chemistry

C–H activation by aqueous platinum complexes: A mechanistic study ☆

G.A. Luinstra, L. Wang, S.S. Stahl, J.A. Labinger *, J.E. Bercaw *

Arnold and Mabel Beckman Laboratories of Chemical Synthesis, California Institute of Technology, Pasadena, CA 91125, USA

Received 19 December 1994; in revised form 17 March 1995

Abstract

Detailed mechanistic studies are reported on the oxidation of alkanes by aqueous $[PtCl_6]^{2-}/[PtCl_4]^{2-}$ to alcohols plus alkyl chlorides, via proposed (alkyl)Pt^{II} and (alkyl)Pt^{IV} intermediates. Reactions of $[PtCl_4]^{2-}$ with RI ($R = CH_3$, CH_2CH_2OH) in water yield $[PtCl_5R]^{2-}$, which were isolated as their NMe_4 salts. Kinetic rate laws of their decomposition in aqueous chloride solution to ROH and RCl support S_N2 displacement by Cl^- or H_2O as the mechanism of the last step. *erythro-* and *threo*-$[PtCl_5(CHDCHDOH)]^{2-}$ are obtained by oxidation of $[PtCl_3$(*trans-* and *cis*-CHD=CHD)$]^-$ respectively, and react with Cl^- with inversion of stereochemistry at carbon, consistent with the S_N2 mechanism. $[PtCl_5(CH_2CH_2OH)]^{2-}$ is also obtained by oxidation of Zeise's salt with $[PtCl_6]^{2-}$. Kinetics indicate that attack of water on coordinated ethylene to give a β-hydroxyethyl group precedes oxidation of Pt^{II} to Pt^{IV}, rather than the reverse order, and that this reaction is a model for the oxidation of (alkyl)Pt^{II} to (alkyl)Pt^{IV} during alkane functionalization. ^{195}Pt isotopic labeling demonstrates that the oxidation is not accompanied by transfer of the β-hydroxyethyl group from one Pt center to another.

Keywords: Platinum; C–H activation

1. Introduction

A great deal of activity has been aimed at discovering and understanding processes of C–H activation by metal complexes during the past decade. The ultimate goal, of course, would be a practical method for functionalization of saturated hydrocarbons. A successful system would have to satisfy (at least) three requirements:

- C–H activation must be part of a catalytic cycle leading to a useful product, not just a stoichiometric transformation.
- Selectivity must be controllable from two points of view: (i) it should be possible to favor the desirable site of attack in a hydrocarbon possessing different C–H bonds; and (ii) the C–H bonds in the product must not be much more reactive than those in the starting hydrocarbon, or low yields will be inevitable.
- Activity be sufficiently high to allow for a practical process under suitably moderate conditions.

Few, if any, of the synthetic systems under study meet all these criteria. Biomimetic catalysts, designed to reproduce the operating principles of biological C–H activators such as cytochrome P-450 or methane monooxygenase, generally appear to follow radical pathways that are not conducive to high selectivity. In contrast, most organometallic C–H activation reactions are certainly non-radical in nature, although the principles governing selectivity are far from clear; and many are remarkably facile, some proceeding rapidly even far below ambient temperatures; but they are not readily incorporated into catalytic cycles.

Our attention was drawn to the so-called electrophilic mode of alkane activation (Eq. (1)), first reported by Shilov and co-workers. The metal complexes involved, chloro(aquo) complexes of Pt(II) and Pt(IV), are much more robust than the typical organometallic species known to react with alkanes via oxidative addition (low-valent late-transition metal complexes) or sigma-bond metathesis (d^0 early transition metal complexes). Closing a cycle to produce a functionalized alkane, as is in fact the case in Eq. 1, rather than an organometallic species should therefore be more feasible.

$$RH + PtCl_6^{2-} + H_2O \xrightarrow[120°C]{PtCl_4^{2-}} ROH + RCl + PtCl_4^{2-} + \ldots . \quad (1)$$

☆ Contribution No. 9027 from the Arnold and Mabel Beckman Laboratories of Chemical Synthesis.

* Corresponding authors.

0022-328X/95/$09.50
SSDI 0022-328X(95)05567-3

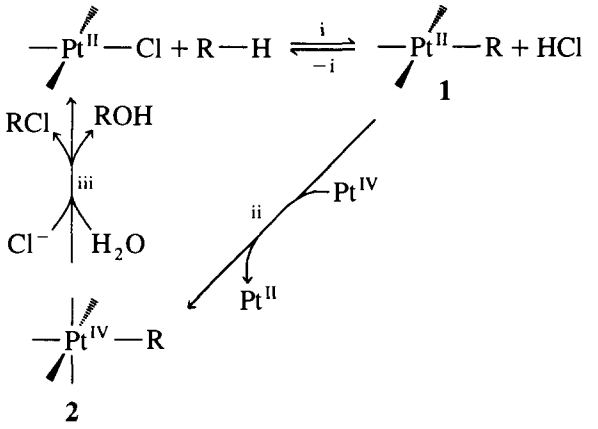

Scheme 1.

Besides this practical motivation, there are important fundamental issues. What is it about these Pt complexes that makes them C–H activators? In contrast to the highly electron-rich complexes that undergo oxidative addition, or the highly electron-deficient complexes that participate in sigma-bond metathesis, these do not appear particularly special in any regard. Why, then, are they capable of effecting such a difficult reaction?

Our initial efforts were concentrated on delineating selectivity patterns and pathways for complex transformations. We found that, in contrast to most previous examples, the products of alkane oxidation are not much more susceptible to further oxidation than the original alkane. The C–H bond in RCH_3 may be even more reactive than in RCH_2OH, permitting such novel transformations as the direct oxidation of ethanol to ethylene glycol with significant selectivity [1,2]. Similar findings have been reported by Sen and co-workers [3]. The potential advantages of the electrophilic route to alkane functionalization may be most clearly seen in the reported conversion of methane to a methanol precursor, catalyzed by Hg^{II}, in over 40% yield [4].

We then turned our attention to the detailed mechanism of C–H functionalization by the mixture of Pt^{II} and Pt^{IV} salts. Our starting point is Shilov's original mechanistic hypothesis, shown in Scheme 1. There are three basic components: (i) C–H activation by Pt^{II} to give an (alkyl)Pt^{II} complex **1**; (ii) reaction of **1** with $PtCl_6^{2-}$ to produce (alkyl)Pt^{IV} **2**; and (iii) reaction of **2** with nucleophile (H_2O or Cl^-) to liberate product (ROH or RCl) and regenerate Pt^{II}. In each case mechanistic alternatives have been proposed, as follows.

(i) Oxidative addition to give $Pt^{IV}(R)(H)$ followed by deprotonation vs. direct deprotonation of the alkane "sigma complex" $Pt^{II}(R–H)$. The latter is attractive by analogy to the well known acidity of dihydrogen complexes, and also as a model agostic complex [5]. This is both the most important (since it presumably governs selectivity and probably also activity) and, unfortunately, the least well understood of the three steps; we do not yet have any definitive mechanistic characterization [6].

(ii) Alkyl transfer from RPt^{II} to Pt^{IV} vs. "simple" oxidation of RPt^{II} by Pt^{IV}. The former would make Pt^{IV} virtually an obligatory oxidant, whereas the latter would permit substitution of alternate oxidants and more readily allow for oxidation catalytic, not stoichiometric, in Pt.

(iii) External nucleophilic attack by X on RPt^{IV} vs. reductive elimination from $Pt^{IV}(R)(X)$. Previous kinetic work supported the former, but it is difficult to reach firm conclusions based on kinetics evidence alone.

In this paper, we report the mechanistic characterization of steps ii and iii, based on studies of kinetics and isotopic labeling in well defined model systems. Preliminary communications of some of these results have appeared previously [7,8].

2. Results and discussion

2.1. Mechanistic study via model systems

Direct study of the alkane functionalization system under operating conditions is difficult for a number of reasons: the starting metal complexes have no convenient NMR handle; distribution among the various species $[Pt^{II}Cl_x(H_2O)_{4-x}]^{(x-2)-}$ and $[Pt^{IV}Cl_x(H_2O)_{6-x}]^{(x-4)-}$ is continuously changing as the reaction proceeds; no organometallic intermediates have yet been isolated from alkane functionalization or even observed in situ [9]. (Alkyl)Pt^{IV} complexes of the type shown as intermediate **2** have been obtained by alternative routes, but intermediate **1**, $[RPt^{II}Cl_x(H_2O)_{3-x}]^{(x-1)-}$, has never been isolated or observed under any conditions. Complexes **1** appear to be susceptible to protonolysis, the reverse of step (i) (see below).

Ligand-substituted analogs of both **1** and **2** are of course very well known, and it is possible to construct a system that reproduces all the features of Scheme 1 except for the initial alkane activation. Such a case is shown in Scheme 2. The (methyl)Pt^{II} complex **3** is readily obtained by controlled protonolysis of $PtMe_2$(tmeda)(Me = CH_3; tmeda = tetramethylethylenediamine). Protonolysis of the second methyl group (step −i) is slower and proceeds at convenient rates around 0°C.

Oxidation of **3** by $[PtCl_6]^{2-}$ in water affords a (methyl)Pt^{IV}(tmeda) complex, most probably $[PtMeCl_2(H_2O)$ (tmeda)]Cl (**4**), based on the ^1H NMR spectrum which shows four separate signals for tmeda methyl groups, two with large ^{195}Pt satellites. Only one of the two tmeda methyl signals in **3** exhibits a large $^3J_{PtH}$, suggesting that the coupling is strongly affected by the nature of the *trans* ligand (methyl vs. chloride), and implying the structure shown for **4**. In

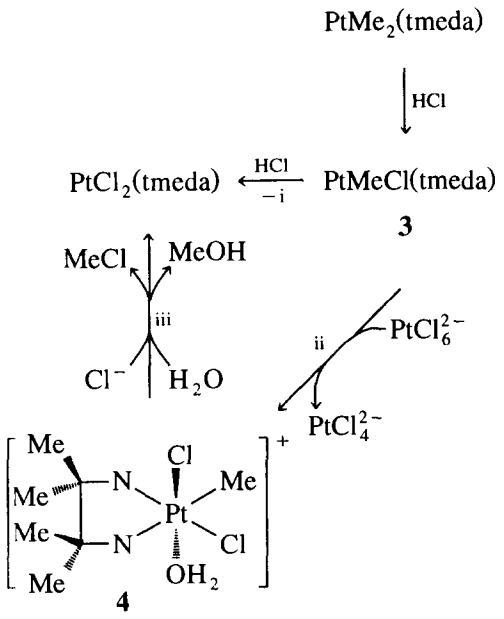

Scheme 2.

contrast, oxidation of **3** by Cl_2 in organic solvents gives a species with only two tmeda methyl signals, presumably $PtMeCl_3$(tmeda). The formation of **4** rather than $[PtMeCl_5]^{2-}$ is consistent with simple oxidation, not alkyl transfer, for step ii. Of course, it is not safe to conclude that the same holds true for the actual alkane activating system, which contains no strongly bound ligands such as tmeda.

Finally, **4** reacts with aqueous chloride at elevated temperatures (but much more slowly than does $[MePtCl_5]^{2-}$; see below) to give methyl chloride and methanol along with $PtCl_2$(tmeda) (step iii). The behavior of this (tmeda) model system thus agrees with Scheme 1, but as the strong tmeda ligand might easily have a major effect, its relevance is not compelling.

2.2. Synthesis and characterization of $[PtMeCl_5]^{2-}$ (5)

Direct study of step iii requires isolation of complexes of type **2**. The synthesis of $M_2[PtRCl_5]$ (M = K, Cs; R = Me, CH_2COCH_3, etc.) has been achieved via oxidative addition of RI to $[PtCl_4]^{2-}$ (Eq. (2)), although products were not obtained in analytically pure form [10]. Isolation of a single product is complicated by the potential for ligand exchange, as Cl^-, I^- and H_2O may substitute for one another. Reaction of $K_2[PtCl_4]$ and MeI in water leads to precipitation of PtI_2, and two Pt(IV)Me complexes according to the ^1H NMR spectra, with $\delta = 3.08$ (major) and 3.10. The relative intensities of the two signals vary from one run to another. The downfield signal appears to be due to an iodo(methyl)Pt^{IV} complex; it disappears on stirring the solution with solid AgCl. This treatment also removes a peak at 430 nm in the visible spectrum; the absence of the latter is a convenient indicator of the purity of $[PtMeCl_5]^{2-}$

$$3[PtCl_4]^{2-} + 2RI \longrightarrow 2[PtRCl_5]^{2-} + PtI_2 + 2Cl^- \quad (2)$$

Filtration and evaporation of the AgCl-treated solution gave a mixture of $K_2[PtMeCl_5]$ and KCl which could not be separated. Therefore, the counterion was changed to tetramethylammonium by ion-exchange column chromatography. Two fractions were obtained, the first containing some of the decomposition product $PtCl_4^{2-}$ (see below) and the other a mixture of NMe_4Cl and $(NMe_4)_2[PtMeCl_5]$. Evaporation and washing with ethanol to remove NMe_4Cl afforded NMR-pure material, as $(NMe_4)_2[PtMeCl_5]$ is very insoluble in ethanol. Analytically pure material was obtained by dissolving the complex in methanol, filtering to remove insoluble $(NMe_4)_2[PtCl_4]$ and adding a saturated methanolic solution of NMe_4Cl.

Alternative routes were less successful. Use of sodium salts throughout resulted in a THF-soluble (alkyl)Pt^{IV} complex which was easily separated from residual NaCl. However, isolation of a solid product proved difficult; only an oily material was obtained unless the THF was rigorously anhydrous and the manipulations were carried out under an inert atmosphere. In that case a yellow solid, probably $Na_2PtMeCl_5$, may be obtained, but it is unstable at room temperature, decomposing overnight in the solid state. A Pt^{IV}–Me complex is also formed in the reaction between methyl tosylate and $K_2[PtCl_4]$ in DMF (choice of the solvent is crucial; no reaction was observed in water, THF or nitromethane). Isolation of a pure compound, however, proved impossible. One of the byproducts, KOTs, could be removed by column chromatography over silica gel, but further attempts to purify the remaining yellow oil only resulted in decomposition.

In aqueous solution, the ^1H and ^{13}C NMR spectra of **5** both show a single peak assignable to Pt-Me, which is not affected by the addition of excess Cl^-; nor is the UV–visible spectrum. In contrast, the ^{195}Pt NMR spectrum shows two signals, at −780 and −822 ppm ($[PtCl_6]^{2-} = 0$), and the relative intensities do depend strongly on $[Cl^-]$; at high chloride concentration the upfield signal becomes dominant. We interpret these observations in terms of the equilibrium shown in Eq. (3), where the signals at −780 and −822 ppm are assigned to **5c** and **5a**, respectively. A rapid equilibrium between **5a** and **5c** would result from dissociative exchange via the five-coordinate intermediate **5b**, facilitated by labilization of the ligand trans to the methyl group. Electrospray ionization mass spectrometry of dilute solutions of **5** show $[PtMeCl_4]^-$ (**5b**) as the only detectable anionic species. The failure to detect this equilibrium by ^1H and ^{13}C NMR indicates that the

resonances are insufficiently sensitive to substitution of water for chloride to resolve, or that the small separation makes the exchange appear fast on the NMR time scale. By measuring the relative intensities of the two ^{195}Pt NMR signals as a function of $[Cl^-]$, we determined the equilibrium constant $K_5 = [\mathbf{5c}]/[\mathbf{5a}]\,[Cl^-] \approx 0.9$ M (at 25°C and ionic strength = 3 M).

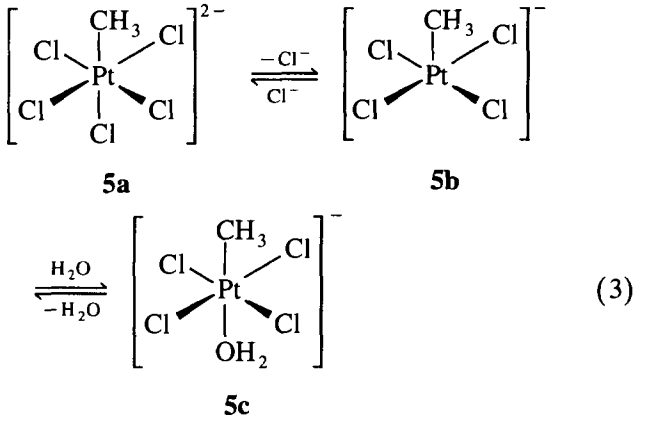

5a **5b**

5c (3)

2.3. Synthesis and characterization of $[Pt(CH_2CH_2OH)Cl_5]^{2-}$ (6)

A (β-hydroxyethyl)Pt^{IV} complex would be the precursor to formation of ethylene glycol from oxidation of ethanol according to Scheme 1; such a species was observed by NMR to result from oxidation of Zeise's salt, $[PtCl_3(C_2H_4)]^-$ (**7**), by Cl_2 in water (Eq. (4)) [11]. The same transformation of **7** to **6** is effected by other oxidants, such as ClO_3^- and H_2O_2 [7], and especially by $[PtCl_6]^{2-}$ (see below). An isolable salt of **6**, though, is most readily obtained by a route analogous to Eq. (2): oxidative addition of 2-iodoethanol to $[PtCl_4]^{2-}$. The same workup procedure was followed; after ion-exchange chromatography a yellow solid was obtained, the NMR and analytical data for which suggested the stoichiometry of a monoanion, $NMe_4[Pt(CH_2CH_2OH)Cl_4]$. Treatment of a methanol solution with excess of NMe_4Cl gave $(NMe_4)_2[Pt(CH_2CH_2OH)Cl_5]$ as an analytically pure orange solid.

$$[PtCl_3(C_2H_4)]^- \xrightarrow{Cl_2/H_2O} [Pt(CH_2CH_2OH)Cl_5]^{2-} + [Pt(CH_2CH_2Cl)Cl_5]^{2-} \quad (4)$$

7 **6**

The ^1H NMR spectrum of **6** shows two triplets, at δ 3.85 and 3.33, as previously reported [11]. In contrast to **5**, however, an additional pair of triplets is observed, about 0.2 ppm upfield from the main signals, for very dilute solutions of **6** at low ionic strength. The identity of the species responsible has not been established; since the methyl complex **5** does not show the same behavior, it is possible that a chelated complex such as

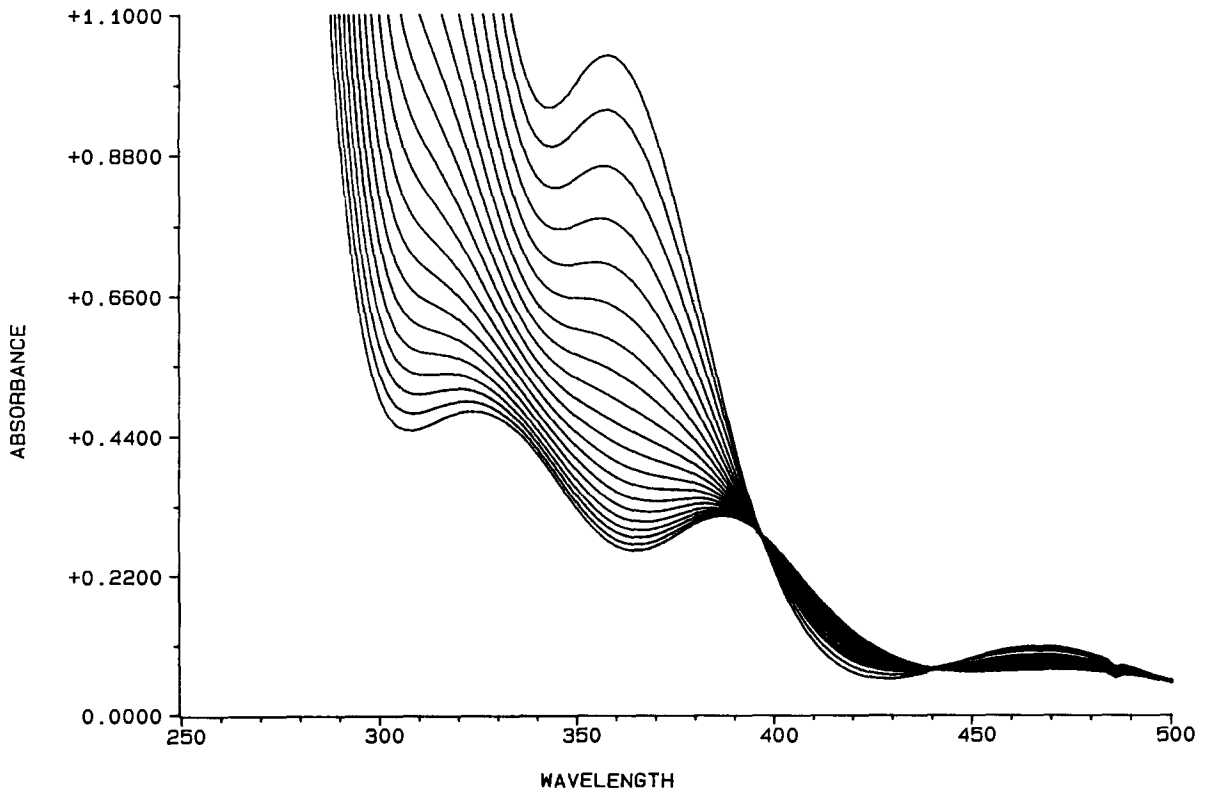

Fig. 1. Changes with time of the UV–visible spectrum of a solution of **5** and Cl^- in H_2O, showing clean isosbestic behavior.

6x is responsible. A related structure could account for the yellow product obtained in the preparation prior to Cl^- addition. The ^{195}Pt NMR behavior, on the other hand, is completely similar to that of **5**: two signals at −731 and −750 ppm are assigned to **6c** and **6a**, respectively, where the structures are as defined by Eq. (3). In this case the measured equilibrium constant $K_6 \approx 0.7$ M.

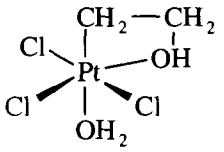

6x

2.4. Kinetics of alkyl chloride / alcohol formation

Although **5** and **6** are reasonably stable in water at room temperature, they decompose slowly at 25°C or more rapidly at elevated temperature according to Eqs. (5) [7,12] and (6) [7,11]. Reactions may be followed either by ^1H NMR (disappearance of the Me-Pt signal) or by UV–visible spectroscopy, taking advantage of the substantial differences in absorbance between Pt^{II} and Pt^{IV}. By either technique the reactions appear clean, with no additional species detectable and good isosbestic behavior followed, as illustrated in Fig. 1. Isosbestic behavior failed only for reactions of **6** at very low $[Cl^-]$, where there is independent evidence for additional species (see above).

$$[PtCH_3Cl_5]^{2-} \xrightarrow{Cl^-/H_2O} CH_3Cl + CH_3OH + [PtCl_4]^{2-} \quad (5)$$

5

$$[Pt(CH_2CH_2OH)Cl_5]^{2-} \xrightarrow{Cl^-/H_2O} ClCH_2CH_2OH + HOCH_2CH_2OH + [PtCl_4]^{2-} \quad (6)$$

6

The kinetics of reactions (5) and (6) were followed by disappearance of the UV–visible absorption (364 nm for **5**; 366 nm for **6**) over a range of $[Cl^-]$, temperature and total ionic strength. Each run showed excellent pseudo-first-order kinetics in total $[Pt^{IV}]$; observed pseudo-first-order rate constants are given in Tables 1 and 2. As $[Cl^-]$ increases, the relative amount of RCl product (vs. ROH) increases, consistent with competitive nucleophilic attack by Cl^- and H_2O. For levels of $[Cl^-] > 0.5$ M, nearly all the observed product from **5** (> 95%) is MeCl. At the same time, the overall rate of decomposition increases, exhibiting saturation kinetics as shown in Fig. 2. There is little or no effect of changing ionic strength from 3 to 6 M, while the rates at 1 M are about two thirds of those at the higher ionic strength levels.

The observed rate constants fit the expression shown in Eq. (7). Such an expression is consistent with the pre-equilibrium of Eq. (3), followed by rate-determining nucleophilic attack on the R group of either the five-coordinate intermediate (**5b**, **6b**) or the six-coordinate aquo complex (**5c**, **6c**), as shown in Scheme 3. The calculated values for k_1, k_2 and K determined by fitting the kinetics to Eq. (7) are shown in Table 3. The numbers are not highly precise, especially for k_2 (which is a relatively minor component of the overall reaction), but the values for K agree to within experimental error with the values for K_5 and K_6 obtained from ^{195}Pt NMR. At first sight that would seem to support the second of the above alternatives, with the limiting rate

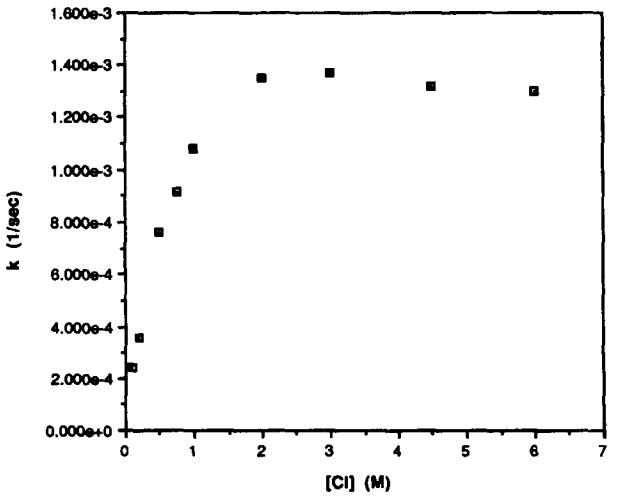

Fig. 2. Apparent first-order rate constant for decomposition of **5** at 45°C as a function of chloride ion concentration.

Table 1
Pseudo-first-order rate constants for the decomposition of $[PtRCl_5]^{2-}$ in aqueous solution at 318 K

R	μ (M)	$[Cl^-]$ (M)	k (s^{-1})
Me	3 [a]	0.12	2.0×10^{-4}
		0.27	4.0×10^{-4}
		0.52	6.3×10^{-4}
		0.77	8.3×10^{-4}
		1.02	9.6×10^{-4}
		1.52	1.15×10^{-3}
		2.02	1.28×10^{-3}
		2.52	1.36×10^{-3}
		3.02	1.39×10^{-3}
Me	6 [a]	0.10	2.4×10^{-4}
		0.20	3.6×10^{-4}
		0.50	7.6×10^{-4}
		0.75	9.1×10^{-4}
		1.00	1.1×10^{-3}
		2.00	1.35×10^{-3}
		3.00	1.37×10^{-3}
		4.50	1.32×10^{-3}
		6.00	1.30×10^{-3}
CH_2CH_2OH	3 [b]	0.10	2.2×10^{-5}
		0.20	2.8×10^{-5}
		0.50	4.5×10^{-5}
		0.75	5.6×10^{-5}
		1.00	6.5×10^{-5}
		2.00	8.7×10^{-5}
		2.50	8.8×10^{-5}

[a] $NaCl–NaClO_4$.
[b] $NaCl–NaNO_3$.

constants extracted from the fit corresponding to the actual rate constants for attack on **5c** and **6c**. In fact, however, as long as the concentration of the five-coordinate intermediate is small the first alternative is equally consistent (see Appendix for derivations). In that case, the apparent calculated rate constants are the actual rate constants divided by K_2, where $K_2 = [\mathbf{5c}]\,[Cl^-]/[\mathbf{5b}]$ (or a corresponding expression for **6**).

$$d[RPt(IV)]/dt = k_{obs}[RPt(IV)];$$

$$k_{obs} = \frac{k_1[Cl^-] + k_2[H_2O]}{1 + K^{-1}[Cl^-]} \quad (7)$$

Although the kinetics do not distinguish, attack on **5b** may be more reasonable on the grounds of microscopic reversibility. Nucleophilic displacement of Pt^{II} from

Table 2
Pseudo-first-order rate constants for the decomposition of $[PtMeCl_5]^{2-}$ in aqueous solution of 1 M ionic strength ($NaCl–NaClO_4$) at various temperatures

$[Cl^-]$ (M)	k (s^{-1})			
	298 K	308 K	318 K	328 K
0.13	8.1×10^{-6}	3.5×10^{-5}	1.4×10^{-4}	4.8×10^{-4}
0.23	1.3×10^{-5}	5.9×10^{-5}	2.1×10^{-4}	7.7×10^{-4}
0.43	2.3×10^{-5}	8.5×10^{-5}	3.5×10^{-4}	12.7×10^{-4}
0.73	3.3×10^{-5}	1.4×10^{-4}	5.2×10^{-4}	19×10^{-4}
1.03	4.1×10^{-5}	1.7×10^{-4}	6.7×10^{-4}	24×10^{-4}

$$[MePtCl_5]^{2-} \overset{K_1}{\rightleftharpoons} [MePtCl_4]^- \overset{K_2}{\rightleftharpoons} [MePtCl_4(H_2O)]^-$$

5a **5b** **5c**

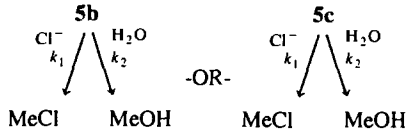

Scheme 3.

RPt^{IV} by X^- is, after all, the reverse of the oxidative addition of RX to Pt^{II}, as shown schematically in Eq. (8). The accepted mechanism for oxidative addition of methyl halides to square-planar d^8 complexes involves a five-coordinate intermediate [13]. The same conclusion was reached in studies on reductive elimination from $PtMe_3I(dppe)$ in acetone: the absence of dependence of rate of MeI formation on $[I^-]$ rules out direct nucleophilic attack on the six-coordinate iodo complex [14].

An important consequence of this mechanism is that it is not safe to deduce anything about mechanism from the dependence of k_1 and k_2 on the structure of R, since the measured numbers incorporate K_2 values which presumably are also sensitive to R. The k_{obs} values for R = Me and R = CH_2CH_2OH are not very different, and the corresponding ethyl compound has been reported to undergo decomposition even faster [15]. These observations appear at first sight to argue against a nucleophilic attack mechanism; but they need not do so, if it is assumed that the bulkier R groups lead to higher concentrations of five-coordinate intermediate (i.e. smaller values of K_2).

$$L_nM + RX \rightleftharpoons [L_nM(R)]^+ + X^- \rightleftharpoons L_nM(R)(X) \quad (8)$$

It *is* possible to compare the ratio of rate constants for attack by chloride and water, k_1/k_2, no matter which mechanism is operative. Precise values are obtained, not from the kinetic expressions but from the relative amounts of RCl and ROH produced as determined by NMR. The ratios thus determined are 4.5×10^3 for **5** and 9.0×10^2 for **6**, both at 45°C. The former value may be compared with that for nucleophilic attack on MeBr, which is 6×10^2 [16]. We also measured the rate of decomposition of **5-d$_3$** and found it to be indistinguishable from protio-**5**; secondary KIEs for S_N2 reactions at methyl are typically in the range 1.0–1.2 [17].

Table 3
Kinetic parameters (as defined in Eq. (7)) for nucleophilic attack on $[PtRCl_5]^{2-}$ at 45°C and μ = 3 M (estimated uncertainty in parentheses)

R	k_1 ($M^{-1}\,s^{-1}$)	k_2 ($M^{-1}\,s^{-1}$)	K^{-1} (M^{-1})
Me	$2.0(1)\times10^{-3}$	$2(1)\times10^{-6}$	1.0(1)
CH_2CH_2OH	$1.0(1)\times10^{-4}$	$2(1)\times10^{-7}$	0.8(1)

The effect of temperature on decomposition of **5** was studied at ionic strength 1 M, to facilitate comparison with alkane activation reactions. This, of course, restricts us to relatively low [Cl^-], where the rate law simplifies to $k_{obs} \approx k_1$ [Cl^-] + k_2, allowing easy extraction of the two rate constants. Eyring plots of both sets of constants were linear and gave activation parameters $\Delta H_1^{\ddagger} = 101$ kJ mol^{-1} and $\Delta S_1^{\ddagger} = 29$ J mol^{-1} K^{-1} (for attack by Cl^-); $\Delta H_2^{\ddagger} = 101$ kJ mol^{-1} and $\Delta S_2^{\ddagger} = 0$ J mol^{-1} K^{-1} (for attack by water). By extrapolation to 120°C, we estimate that the half-life of **5** under conditions where alkane activation takes place should be well under 1 s, making it questionable whether sufficient concentrations for observation would accumulate [9].

2.5. Reactions of other nucleophiles

Addition of excess $NaNO_2$ to a solution of **5** leads to immediate appearance of new signals in the ^1H (δ 2.93) and ^{195}Pt (δ − 827) NMR spectra. Presumably this corresponds to the equilibrium shown in Eq. (9); the ^{195}Pt NMR intensities give a value of $K \approx 8$–10 M^{-1}, indicating that NO_2^- is a better ligand than Cl^-. On warming to 45°C, both MeOH and $MeNO_2$ are formed.

$$[PtMeCl_4(H_2O)]^- + NO_2^- \rightleftharpoons [PtMeCl_4(NO_2)]^{2-} + H_2O \quad (9)$$

No reaction of **5** is observed on dissolution in aqueous phosphate buffer (pH 6) at room temperature; but warming to 45°C results in both a new $MePt^{IV}$ resonance (δ 2.9) and formation of methyl phosphate (δ 3.4, $^3J_{PH} = 12$ Hz). Similarly, **5** reacts with aqueous NaF only on warming to 45°C, giving a new complex (^1H δ 2.95; ^{195}Pt δ − 191) but no MeF. The formation of MeX in each case must depend on both the nucleophilicity of X-towards the Me–Pt bond and the affinity of X for Pt (which governs the concentration of the reactive five-coordinate intermediate). No detailed kinetics have yet been carried out for these reactions.

2.6. Mechanism of the oxidation of Zeise's salt (7) by $[PtCl_6]^{2-}$

As noted above, **6** may be obtained by oxidation of Zeise's salt. Whereas the use of Cl_2 as oxidant gives a mixture of **6** and the analogous (chloroethyl)Pt^{IV} complex (Eq. (4)) [11], $[PtCl_6]^{2-}$ oxidizes **7** cleanly to **6** as sole product (Eq. (10)). This reaction is important for three reasons: it is implicated as a key step in the oxidation of ethanol to ethylene glycol [2]; it provides a route to stereolabeled **6** for further probing step iii (see below); and it may serve as a model for step ii, the oxidation of an alkylPt^{II} complex.

$$[PtCl_3(C_2H_4)]^- + [PtCl_6]^{2-} + H_2O \xrightarrow[\textbf{7}]{} [Pt(CH_2CH_2OH)Cl_5]^{2-} + [PtCl_4]^{2-} + H^+ \quad (10)$$

(**6**)

The last statement is qualified because, in principle, the conversion of **7** to **6** could take place by either of two sequences: addition of water to **7** to give a (hydroxyethyl)Pt^{II} complex followed by oxidation (Eqs. (11) and (12)); or the reverse, oxidation to an (ethylene)Pt^{IV} complex followed by hydration (Eqs. (13) and (14)). Further, any of the steps might be reversible.

$$[PtCl_3(C_2H_4)]^- + H_2O \xrightarrow[\textbf{7}]{} [Pt(CH_2CH_2OH)Cl_3]^{2-} + H^+ \quad (11)$$

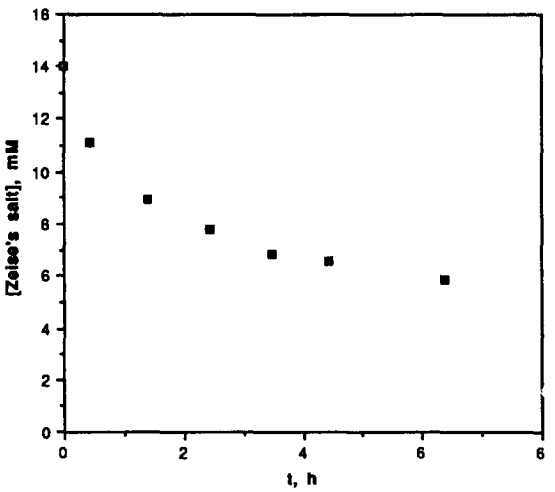

Fig. 3. Concentration of Zeise's salt (**7**) vs. time in reaction with $[PtCl_6]^{2-}$.

$$[Pt(CH_2CH_2OH)Cl_3]^{2-} + [PtCl_6]^{2-} \longrightarrow [Pt(CH_2CH_2OH)Cl_5]^{2-} + [PtCl_4]^{2-} \quad (12)$$

6

$$[PtCl_3(C_2H_4)]^- + [PtCl_6]^{2-}$$

7

$$\longrightarrow [PtCl_5(C_2H_4)]^- + [PtCl_4]^{2-} \quad (13)$$

$$[PtCl_5(C_2H_4)]^- + H_2O \longrightarrow [Pt(CH_2CH_2OH)Cl_5]^{2-} + H^+ \quad (14)$$

6

Our initial kinetic studies strongly implied that a reversible step is involved: the dependence on [7] exhibits behavior suggesting an approach to equilibrium (Fig. 3). It is easy to show that the overall reaction is not reversible, as a solution containing **6** and $[PtCl_4]^{2-}$ remains unchanged over several hours at 45°C. It can also be demonstrated that Eq. (14), if it operates, is not reversible. Regiospecifically deuterated **6** was prepared by oxidative addition of ICH_2CD_2OH to $[PtCl_4]^{2-}$; the ^1H NMR spectrum shows only the signal expected, corresponding to the methylene group adjacent to Pt, even after 8 h in solution at 45°C. A reversible Eq. (14) would scramble the two methylene positions.

Of the remaining possibilities, reversible (11) followed by irreversible (12), irreversible (11) followed by reversible (12) and reversible (13) followed by irreversible (14), the last two require that the reaction be slowed in the presence of excess $[PtCl_4]^{2-}$. In fact, addition of $[PtCl_4]^{2-}$ has no effect on the rate of Eq. (10). The only possibility left requires inhibition by added H^+, which *is* found: at pH < 1 the reaction is too slow to follow at 45°C. It can be monitored at 85°C, but at that temperature the subsequent decomposition of **6** is fast, and only the final products $ClCH_2CH_2OH$ and $HOCH_2CH_2OH$ are observed. Nonetheless, it is possible to follow disappearance of **7**, which is first-order in both [7] and $[PtCl_6]^{2-}$ and inverse first-order in $[H^+]$ (Table 4), consistent with Eqs. (15)–(17).

$$[PtCl_3(C_2H_4)]^- + H_2O$$

7

$$\overset{K}{\rightleftharpoons} [Pt(CH_2CH_2OH)Cl_3]^{2-} + H^+ \quad (15)$$

8

$$[Pt(CH_2CH_2OH)Cl_3]^{2-} + [PtCl_6]^{2-} \overset{k}{\longrightarrow} [Pt(CH_2CH_2OH)Cl_5]^{2-} + [PtCl_4]^{2-} \quad (16)$$

6

$$d[7]/dt = -kK[7][PtCl_6]^{2-}/[H^+] \quad (17)$$

Table 4
Pseudo-first-order rate constants for the oxidation of Zeise's salt (7) with $[PtCl_6]^{2-}$ at 85°C

$[PtCl_6^{2-}]$ (M)	$[D^+]$ (M) [a]	μ (M) [b]	k_{obs} (s^{-1})
0.1	0.13	2.2	4.0×10^{-5}
0.2	0.13	2.3	8.0×10^{-5}
0.4	0.13	2.0	1.9×10^{-4}
0.6	0.13	2.3	3.0×10^{-4}
0.2	0.27	2.3	4.1×10^{-5}
0.4	0.27	2.5	8.8×10^{-5}

[a] $[D^+]$ determined with a pH meter; glass electrode previously exchanged by soaking in 2 M $KCl-D_2O$.
[b] $NaCl-NaClO_4$.

The data in Table 4 provide only a very narrow range in $[H^+]$, since $[H^+]$ must be kept high if it is to remain essentially constant over the course of the reaction. A much wider range should be attainable in buffered solutions; unfortunately, we have not yet been able to find a buffer system that does not interfere with the course of oxidation. In phosphate buffer at pH ≈ 6, **7** is consumed much faster than in plain water, and no **6** is produced. In contrast, using $ClCH_2COOH/ClCH_2COO^-$ at pH 1.8–8.3 oxidation is independent of pH but strongly dependent on buffer concentration, suggesting that $ClCH_2COO^-$ catalyzes the oxidation of **7** by $[PtCl_6]^{2-}$.

To confirm the H^+ dependence, we carried out kinetics in neutral (pH 7) aqueous solution, obtaining data of the sort shown in Fig. 3. Since $[H^+] = [7]_0 - [7]$ (where $[7]_0$ is the initial concentration of Zeise's salt), substitution into Eq. (17) and integration (see Appendix) gives the rate law shown as Eq. (18). When data for concentration of **7** are transformed according to the left-hand side of the equation and plotted against time, good straight lines are obtained (Fig. 4). The composite rate constants, kK, derived from that procedure are shown in Table 5. It may be noted that the reaction is slowed

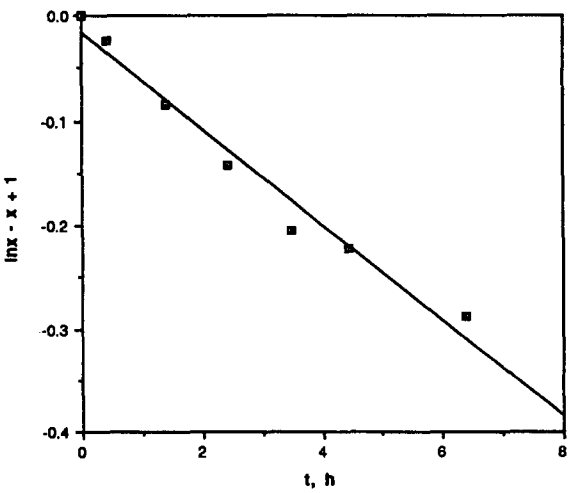

Fig. 4. Data from Fig. 3 plotted according to Eq. (18) ($x = [7]/[7]_0$).

Table 5
Rate constants (kK) determined from fitting data to Eq. (18) for the oxidation of Zeise's salt (**7**) to $PtCl_5CH_2CH_2OH$ (**6**) by $PtCl_6^{2-}$ at 45°C, $\mu = 3.3 \pm 0.3$ M

[7] (M)	$[PtCl_6^{2-}]$ (M)	$[Cl^-]$ (M)	c (s^{-1}) [b]	kK (s^{-1})
0.014	0.14	0.3	8.7×10^{-6}	8.7×10^{-7}
0.014	0.14	0.6	7.4×10^{-6}	7.4×10^{-7}
0.014	0.14	1.0	5.0×10^{-6}	5.0×10^{-7}
0.014	0.14 [c]	1.0	4.8×10^{-6}	4.8×10^{-7}
0.014	0.28	1.0	8.1×10^{-6}	4.1×10^{-7}
0.014	0.56	1.0	1.6×10^{-5}	4.0×10^{-7}
0.028	0.28	1.0	4.7×10^{-6}	4.7×10^{-7}
0.056	0.56	1.0	4.3×10^{-6}	4.3×10^{-7}
0.014	0.14	2.0	5.0×10^{-6}	5.0×10^{-7}
0.014	0.28	2.0	1.2×10^{-5}	6.0×10^{-7}
0.014	0.14	3.0	4.6×10^{-6}	4.6×10^{-7}
0.014	0.28	3.0	1.1×10^{-5}	5.5×10^{-7}
0.014	0.56	3.0	1.7×10^{-5}	4.3×10^{-7}
0.056	0.56	3.0	4.0×10^{-6}	4.0×10^{-7}

[a] $NaCl$–$NaClO_4$.
[b] Slope of line plotted according to Eq. (18).
[c] 0.14 M $[PtCl_4]^{2-}$ added.

somewhat by high levels of Cl^-, although there is virtually no effect of total ionic strength [18].

$$\ln([7]/[7]_0) - ([7]/[7]_0) + 1 = -kK\left([PtCl_6]^{2-}/[7]_0\right)t \equiv -ct \quad (18)$$

Hutson et al. [19] noted that no hydrated product can be observed when Zeise's salt is exposed to high pH, which requires that the equilibrium in Eq. (15) lies far to the left. Why, then, is **7** not directly oxidized? Presumably this is related to the stabilization of Pt^{II} by the π-acceptor ligand ethylene. The (hydroxyethyl)Pt^{II} intermediate **8**, even though present in very low concentration, must be remarkably rapidly oxidized. There is independent evidence that the oxidation of RPt^{II} by $[PtCl_6]^{2-}$ is fast: nucleophilic attack by Cl^- on the (dimethyl)Pt^{IV} complex **9** produces MeCl, with (methyl)Pt^{II} complex **10** the presumed coproduct (Eq. (19)). The latter is completely protonolyzed to methane

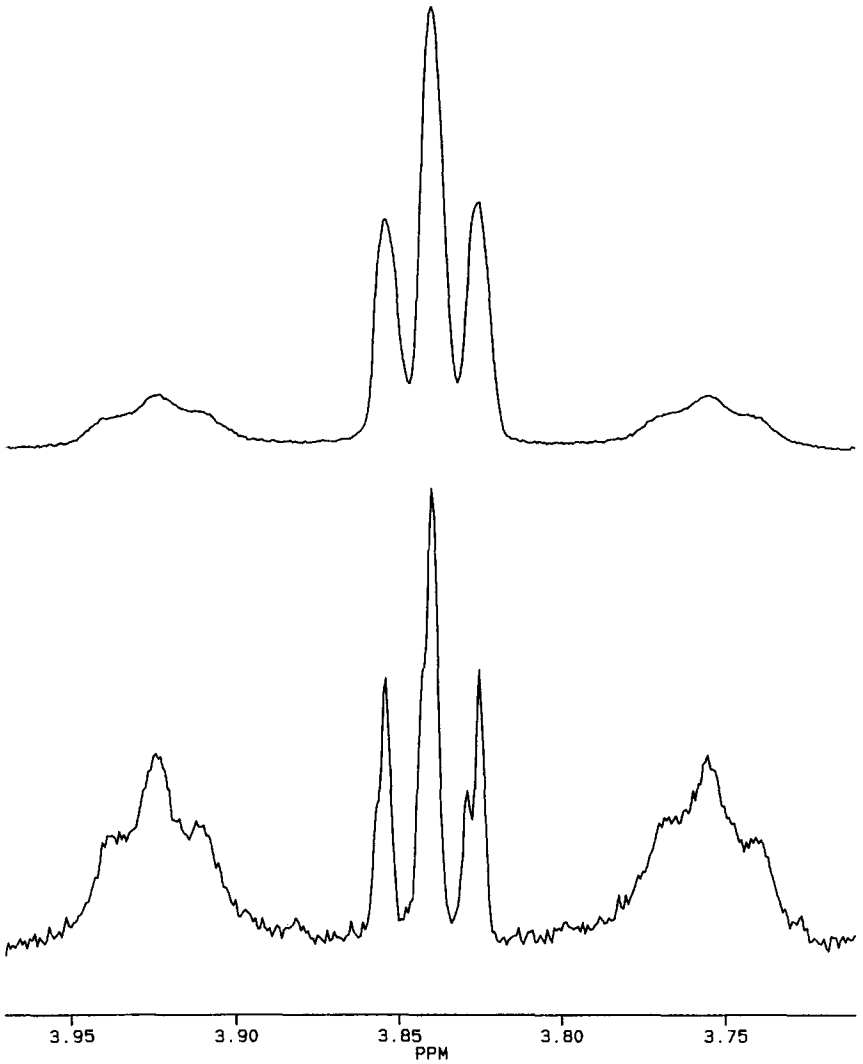

Fig. 5. Pt(CH_2CH_2OH) signal in the ^1H NMR spectrum of **6** generated by oxidation of Zeise's salt with $[^{195}PtCl_6]^{2-}$. Top, 24 h after reaction complete; bottom, 34 days later.

unless $[PtCl_6]^{2-}$ is also present in solution, in which case there is competitive oxidation to **5** [20]. We can generate **10** by reducing **5** with Cr^{II} or Sn^{II} and find that methane is liberated instantaneously even at 0°C; since protonolysis is extremely fast, so also must be oxidation.

$$[PtMe_2Cl_4]^{2-} + Cl^- \xrightarrow{95°C} MeCl + [PtMeCl_3]^{2-} \xrightarrow{[PtCl_6]^{2-}} [PtMeCl_5]^{2-} \quad \mathbf{5}$$
$$\xrightarrow{H^+} MeH \qquad (19)$$

2.7. Oxidation by isotopically enriched $[PtCl_6]^{2-}$. Alkyl vs. Electron Transfer

Since oxidation of Zeise's salt by $[PtCl_6]^{2-}$ proceeds via an (alkyl)Pt^{II} intermediate, it can serve as a model for step ii of the overall functionalization mechanism, and we can use it to determine whether the alkyl group is transferred between Pt centers as proposed. Isotopically enriched ^{195}Pt(97.3%) was purchased, dissolved in aqua regia, converted into $Na_2[^{195}PtCl_6]$, and reacted with natural abundance **7**. If the alkyl group undergoes transfer to the Pt^{IV} center during oxidation, the resulting **6** should be highly enriched in ^{195}Pt, which would be readily detected from the intensity of the satellites of the $PtCH_2CH_2OH$ ^1H NMR signal. In fact, the initial spectrum shows satellites of normal intensity (ca. 33% of total peak area), as shown in Fig. 5; the oxidation proceeds according to Eq. (20). Hence the oxidation does not involve alkyl transfer; as discussed earlier, an inner-sphere two-electron transfer accompanied by Cl transfer is the probable mechanism.

$$[PtCl_3(C_2H_4)]^- + [^{195}PtCl_6]^{2-}$$
$$\mathbf{7}$$
$$\xrightarrow{H_2O} [Pt(CH_2CH_2OH)Cl_5]^{2-} + [^{195}PtCl_4]^{2-}$$
$$\mathbf{6} \qquad (20)$$

It may be seen in Fig. 5 that the satellite peaks gradually increase if the solution is allowed to stand for several days at room temperature. This could be due to exchange of the alkyl group between **6** and either uncreacted $[^{195}PtCl_6]^{2-}$ or coproduct $[^{195}PtCl_4]^{2-}$. Separate experiments using isolated **5** or **6** and one of the two oxidation states of the labeled complex demonstrate that the alkyl group transfers only to Pt^{II} (Eq. (21)). This is best understood as an S_N2 reaction, with $[PtCl_4]^{2-}$ acting as both nucleophile and leaving group. In like fashion, $[PtCl_4]^{2-}$ reacts with **9** to give **5** (Eq. (22)) [20]. (It is attractive and perhaps useful to think of $[MePtCl_5]^{2-}$ and $[PtCl_4]^{2-}$ as respectively analogs of MeI and I^-!)

$$[Pt(CH_2CH_2OH)Cl_5]^{2-} + [^{195}PtCl_4]^{2-}$$
$$\mathbf{6}$$
$$\xrightarrow{slow} [^{195}Pt(CH_2CH_2OH)Cl_5]^{2-} + [PtCl_4]^{2-} \qquad (21)$$

$$[PtMe_2Cl_4]^{2-} + [PtCl_4]^{2-}$$
$$\mathbf{9}$$
$$\longrightarrow [PtMeCl_3]^{2-} + [PtMeCl_5]^{2-}$$
$$\mathbf{10} \qquad \mathbf{5}$$
$$\longrightarrow MeH + MeCl \qquad (22)$$

By following the growth in intensity of the satellite peaks we can determine the extent of exchange as a function of time, and plotting the data according to the expected expression for approach to equilibrium by second-order kinetics gives good straight lines, from which the apparent second-order rate constant k_{obs} is extracted. Following the analysis for nucleophilic attack by Cl^- we obtain the expression $k_{obs} = (k_{exch}/K_2)/(1 + [Cl^-]/K)$, where K and K_2 are the same as before. In the absence of added Cl^- the denominator will be close to 1 ($[Cl^-]$ is small and $K \approx 1$), so k_{obs} may be compared directly with k_1 to give the relative nucleophilicity of Cl^- and $[PtCl_4]^{2-}$ towards RPt^{IV}.

Table 6 lists rate constants for nucleophilic attack by Cl^- and $[PtCl_4]^{2-}$ on **5**, **6** and **9**. Several interesting trends are clear. First, $[PtCl_4]^{2-}$ is a much better nucleophile than Cl^- towards Me-Pt. For both (monomethyl)Pt^{IV} **5** and (dimethyl)Pt^{IV} **9** the rate constant ratio k_{exch}/k_1 is about 100. In contrast, the ratio is only about 5 for nucleophilic attack on (β-hydroxyethyl)Pt^{IV} **6** (assuming the activation parameters for **6** + Cl^- are about the same as for **5**). Presumably this reflects a much greater sensitivity to steric effects for nucleophilic attack by $[PtCl_4]^{2-}$ than by Cl^-. Another way of putting this is that the ratio of rates for attack by $[PtCl_4]^{2-}$ on **5** vs. **6** is around 1700. Finally, the (dimethyl)Pt(IV)

Table 6
Apparent second-order rate constants for nucleophilic attack on alkylPt^{IV} complexes.

MePt complex	Nucleophile	T (°C)	k (M^{-1} s^{-1})
$[PtMeCl_5]^{2-}$ (**5**)	Cl^-	45	2.0×10^{-3}
		20	5.5×10^{-5} [a]
		95	2.9×10^{-1} [a]
	$[PtCl_4]^{2-}$	22	1.9×10^{-2} [b]
$[PtCl_5CH_2CH_2OH]^{2-}$ (**6**)	Cl^-	45	1.0×10^{-4}
	$[PtCl_4]^{2-}$	20	1.1×10^{-5} [b]
$[PtMe_2Cl_4]^{2-}$ (**9**)	Cl^-	95	3.2×10^{-6} [c]
	$[PtCl_4]^{2-}$	95	2.7×10^{-4} [c]

[a] Calculated from 45°C data and activation parameters.
[b] From ^{195}Pt exchange between **5** or **6** and $[PtCl_4]^{2-}$.
[c] Ref. [20].

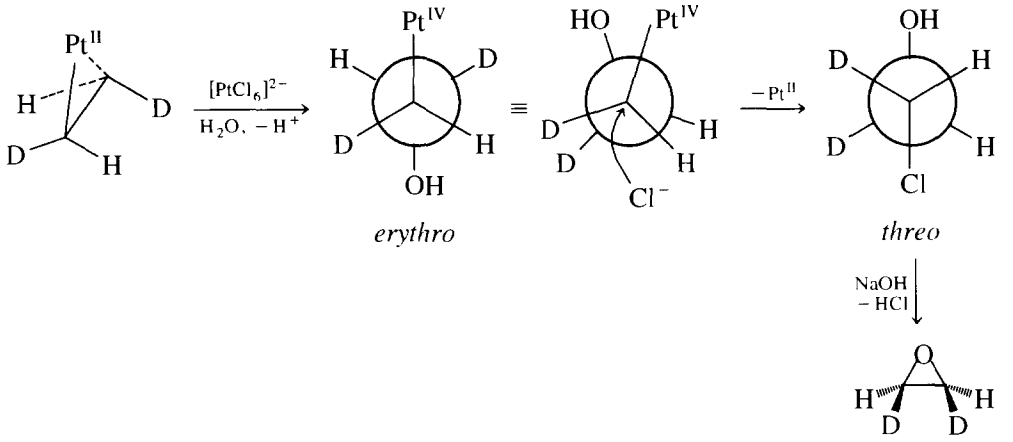

Scheme 4.

complex is much less susceptible to nucleophilic attack than its monomethyl counterpart. Possible explanations include the relative tendency to dissociate a ligand (unknown), the increased stability of higher oxidation states with methylation and the instability of leaving group $[Pt^{II}MeCl_3]^{2-}$ (the latter two are related).

2.8. Stereochemistry of formation of RCl from RPt^{IV}

While the rate law and some of the reactivity trends are consistent with nucleophilic displacement, it is difficult to exclude conclusively alternatives such as reductive elimination. The most definitive demonstration of an S_N2 mechanism is inversion of configuration at carbon. A suitable test compound is obtained by oxidation of Zeise's salt prepared from *cis*- or *trans*-1,2-dideuterioethylene, which leads to (predominantly) *threo*- or *erythro*-$[Pt(CHDCHDOH)Cl_5]^{2-}$ (**6-d$_2$**), respectively (Eq. (23)). These transformations are only about 85–90% stereospecific, as determined from the ^1H NMR spectrum. Thus, when starting from *trans*-**7-d$_2$**, the PtC*H*DC*H*DOH signals of **6** may be resolved into two sets of doublets, with $^3J_{HH} \approx 8$ Hz (85–90%) and 6 Hz (10–15%), assigned to the *erythro* and *threo* isomers, respectively. (All-protio **6** exhibits apparent triplets, $^3J_{HH} \approx 7$ Hz, for the two CH_2 signals [11].) This indicates that formation of (hydroxyethyl)Pt^{II} arises mostly from attack of external water on the olefin (trans addition) but with some contribution from olefin insertion into a Pt–OH bond (cis addition), as is also found in Wacker chemistry [21].

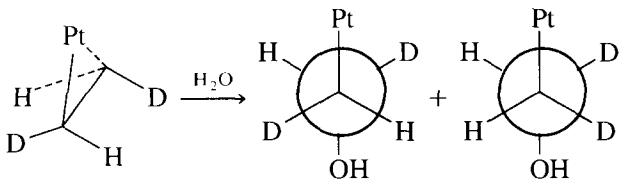

trans *erythro* 85–90% *threo* 10–15%

(23)

The labeled **6-d$_2$** complexes react with aqueous chloride, as described earlier, to give a mixture of ClCHDCHDOH and HOCHDCHDOH. Stereochemical information is lost in the latter product, but the former reveals that the reaction goes with predominant inversion: *erythro*-**6-d$_2$** gives primarily *threo*-ClCHDCHDOH ($^3J_{HH} = 6$ Hz) and vice versa. The resolution of signals is not good enough to determine the degree of stereospecificity, so the chloroethanol was treated with NaOH to convert it into ethylene-d_2 oxide, which can be analyzed more precisely by IR spectroscopy [22]. The epoxide obtained from (predominantly) *erythro*-**6-d$_2$** was found to be 85 ± 5% cis, which is consistent with 100% inversion in the formation of ClCHDCHDOH (Scheme 4). Along with the kinetics, this finding provides very strong support for an S_N2 mechanism. (Intramolecular reductive elimination of ethylene oxide — with retention — followed by ring-opening attack by Cl^- could also account for net inversion in formation of ClCHDCHDOH from **6-d$_2$**. However, this alternative is ruled out by the observation that $[Pt(CH_2CD_2OH)Cl_5]^{2-}$ reacts with Cl^- to give only $ClCH_2CD_2OH$. If ethylene oxide were an intermediate, an equal amount of $ClCD_2CH_2OH$ would form.)

We also briefly examined the oxidation of Zeise's salt by Cl_2. As initially reported by Halpern and Jewsbury [11], the reaction takes place stepwise: very rapid formation of $[Pt(CH_2CH_2Cl)Cl_5]^{2-}$ (**11**), followed by slow (at room temperature) solvolysis to **6** and even slower cleavage to give $ClCH_2CH_2OH$ and small amounts of ethylene glycol. The second step was proposed to occur via nucleophilic displacement, accelerated by the β-Pt substituent. However, when the reaction is carried out with **6-d$_2$**, retention of stereochemistry is observed: *cis*-**7-d$_2$** leads to *threo*-**11-d$_2$** and thence to *threo*-**6-d$_2$**. This result is inconsistent with an S_N2 displacement, and suggests instead an (ethylene)Pt^{IV} intermediate (Eq. (24)). If so, the addition of water to the latter must be virtually completely *trans*, in contrast to the analogous reaction of (ethylene)Pt^{II}, which is only 85–90% stereospecific.

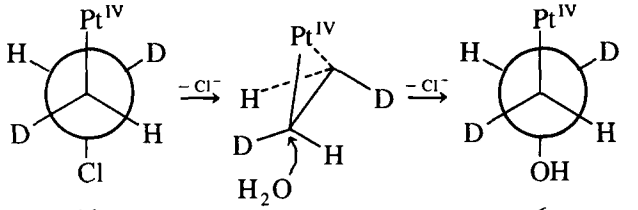

11 **6** (24)

It is also noteworthy that no 1,2-dichloroethane, which should arise from attack of Cl^- on **11**, was observed to result from oxidation of **7** by Cl_2 [11]. One possibility is that **6** or **11** only undergoes nucleophilic attack in a particular rotomer, **12g**. The difference between *gauche* and *trans* coupling constants in **11** (4 and 14 Hz, respectively, as measured for the d_2 isomers; values of 4 and 13 Hz were determined by fitting the AA'XX' patterns of all-protio **11** [11]) is much larger than in **6** (6 and 8 Hz), implying that the conformational preference for **12t** is considerably greater in the former, so access to the reactive conformation is effectively prevented.

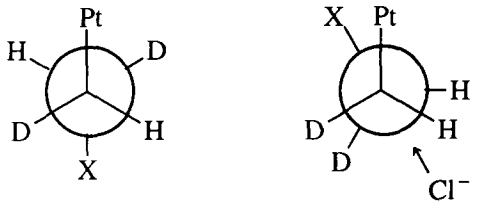

12t (X = Cl, OH) **12g**

3. Summary and conclusions

Our results are fully consistent with the three-step mechanism for functionalization of C–H bonds: formation of an (alkyl)Pt^{II} complex, oxidation to (alkyl)Pt^{IV} and cleavage of the C–Pt^{IV} bond to liberate product and regenerate Pt^{II}. The natures of the second and third steps are revealed by kinetics, isotope labeling and stereochemistry to proceed by electron transfer (not alkyl transfer) and nucleophilic attack (not reductive elimination), respectively.

What is it about this particular system that allows it to carry out functionalization of alkanes? While the details of the first step, the actual C–H activation by the Pt^{II}/Pt^{IV} system, have not yet been fully elucidated, it seems clear that a key factor in the overall mechanism is the versatility of the Pt^{II} center, which can behave both as an effective electrophile/electrofuge and as a nucleophile/nucleofuge. Thus we see that RPt^{II} is readily susceptible to (electrophilic) protonolysis, whereas RPt^{IV} is stable even to 1 M acid. In contrast, RPt^{IV} undergoes nucleophilic attack, with Pt^{II} as the leaving group. This modulation of the reactivity of the RPt center by oxidation must play an important role in the overall sequence of alkane functionalization. C–H activation by Pt^{II} is formally the microscopic reverse of protonolysis of RPt^{II}, so electrophilic character is required at the outset. Oxidation to RPt^{IV} both protects the organometallic intermediate against rapid reversion by protonolysis and converts it into a form that favors formation of the target C–X bond.

Clearly, oxidation of RPt^{II} must be fast to compete with protonolysis, and oxidation by Pt^{IV} has been shown to be very rapid [20]. However, the fact that the second step does not involve alkyl transfer to Pt^{IV} suggests that the latter is not an essential component. Indeed, it can be replaced by alternate oxidants, such as O_2 [23] or electrochemical oxidation [24] (in each case a heteropolyanion is required as electron-transfer mediator), to achieve alkane oxidation catalytic in Pt^{II}, although only a few turnovers have yet been achieved.

Obviously a number of important questions remain unanswered. These include: how does the initial C–H activation take place?; what is the mechanistic connection between this system and others (e.g. the mercury system mentioned earlier [4]) that carry out apparently related chemistry?; how might the system be improved in terms of activity, selectivity and catalytic potential? Work aimed at providing some answers is in progress.

4. Experimental section

4.1. Materials and methods

Platinum salts were obtained from Aldrich, with the exception of Na_2PtCl_4, which was obtained from Aesar. DMF was dried over lithium aluminum hydride and distilled. THF was distilled from Na–benzophenone. All others reagents were obtained commercially and used without further purification.

NMR spectra were recorded on General Electric QE300, Jeol FNM400 and Bruker AM500 spectrometers. Infrared spectra were recorded on a Perkin-Elmer 1600 series FTIR spectrometer. Gas chromatograms were recorded on a Perkin-Elmer 8410 gas chromatograph (Carbowax 20M column). UV–visible spectra were recorded on a HP 8452A spectrophotometer; the cuvet holder was electronically thermostated with an HP 89090A instrument (Peltier element). Microanalyses were performed by Galbraith Laboratories or Fenton Harvey of this department; values are the averages of two independent determinations. Ion exchanges were performed on a chromatographic column (i.d. 1 cm) prepared by charging with 5 g of cation-exchange resin (Bio-Rad AG 50W-X2, 50–100 mesh, 5.2 mequiv., g^{-1}, hydrogen form) and treating with a solution prepared from 6 g of NMe_4OH in 150 ml of water. Subsequently, the column was washed with deionized water until the eluate had pH 7.

4.2. Preparation of PtMeCl(tmeda) (3)

$PtMe_2$(tmeda) was prepared according to literature procedures [25]. The crude product (196 mg, ca. 0.57 mmol) was dissolved in a mixture of CH_2Cl_2 (8 ml) and CH_3OH (3 ml) in a small flask containing a stirrer bar. Acetyl chloride (40.8 μl, 0.57 mmol) was added slowly to the stirred reaction mixture. After a short induction period gas evolution was observed, and the reaction mixture was stirred for a further 1 h. After removing the solvent under vacuum, the product was purified by successive dissolution in warm CH_2Cl_2 and precipitation by addition of diethyl ether. The product was obtained as a white to off-white powder. Yield: 125 mg, 0.34 mmol (60%). Anal. ($C_7H_{19}N_2ClPt$). Calc.: C, 23.24; H, 5.29; N, 7.74. Found: C, 23.41; H, 5.43; N, 7.78%. ^{1}H NMR (CD_2Cl_2, 25°C): δ 2.84 (s, ^3JPt–H = 51.4 Hz, Pt-N-CH_3), 2.77 (m, Pt-N-CH_2–), 2.70 (s, ^3JPt–H < 10 Hz, Pt-N-CH_3), 2.54 (m, Pt-N-CH_2–), 0.434 (s, ^2JPt–H = 78.9 Hz, Pt-CH_3). ^{13}C NMR (CD_2Cl_2, 25°C): δ 66.52 (s, tmeda), 60.46 (s, tmeda), 52.30 (s, tmeda), 48.69 (s, tmeda), −22.53 (s, Pt-CH_3).

4.3. Protonolysis of PtMeCl(tmeda) by HCl(g)

PtMeCl(tmeda) (30 mg, 0.083 mmol) was placed in a flask with a stirrer bar and and dissolved in CH_2Cl_2 (5 ml). The solution was degassed on a high-vacuum line and HCl(g) (6.9 ml, 298 K, 22.4 Torr, 0.083 mmol) was transferred into the reaction flask using a gas bulb. The solution was stirred for 1 h, during which time gas evolution was apparent. The gas was collected and quantified with the Toepler pump and characterized as CH_4 by IR spectroscopy. The pale-yellow $PtCl_2$(tmeda) remaining in the reaction mixture was characterized by comparing its ^{1}H NMR spectrum with that of an authentic sample. The identical reaction also occurs in other solvents (e.g. H_2O and MeOH).

4.4. Oxidation of 3 by $PtCl_6^{2-}$

Solid K_2PtCl_6 (32 mg, 0.066 mmol) was added to an aqueous suspension of **3** (21 mg, 0.058 mmol) and the mixture was stirred vigorously for ca. 10 min. Subsequent addition of CH_2Cl_2 and vigorous stirring resulted in extraction of a "Pt^{IV} Me(tmeda)" species from the aqueous $PtCl_6^{2-}/PtCl_4^{2-}$ solution. ^{1}H NMR data are most consistent with the product formulation: [$PtMeCl_2(H_2O)$(tmeda)]Cl (**4**). The product was purified by recrystallization from CH_2Cl_2–Et_2O. ^{1}H NMR (D_2O, 25°C): δ 2.88 (m, Pt-N-CH_2–), 2.78 (m, Pt-N-CH_2–), 2.72 (m, Pt-N-CH_2–), 2.63 (s, Pt-N-CH_3, ^3JPt–H = < 10 Hz), 2.56 (s, Pt-N-CH_3, ^3JPt–H = 35.8 Hz), 2.45 (s, Pt-N-CH_3, ^3JPt–H = < 10 Hz), 2.30 (s, Pt-N-CH_3, ^3JPt–H = 30.5 Hz), 2.05 (s, Pt-CH_3, ^2JPt–H = 68.3 Hz).

4.5. Reaction of [$PtMeCl_2(H_2O)$(tmeda)]Cl (4) with chloride

In a 5 mm NMR tube, **4** (1.5 mg, 3.5×10^{-3} mmol), excess NaCl (50 mg, 0.86 mmol) and D_2O (0.5 ml) were combined. The tube was sealed and heated at 120°C in an oil-bath. Disappearance of **4** (by ^{1}H NMR) was complete after ca. 32 h, producing $PtCl_2$(tmeda) and CH_3OH.

4.6. Synthesis of $K_xCl_yPt(CH_3)$

K_2PtCl_4 (4.0 g, 9.6 mmol) was suspended in 50 ml of water. CH_3I (500 ml, 8 mmol) was added and a brownish black precipitate soon formed. After stirring for 6 h, the water was removed under vacuum and the residue extracted with methanol until washings were colorless (ca. 500 ml). After evaporation to dryness of the methanolic solution, 1.9 g of a dark-yellow powder remained. $AgNO_3$ (3.0 g) was dissolved in water and treated with 5 ml of concentrated HCl. The solid AgCl thus formed was thoroughly washed with water to remove excess chloride. The yellow powder was dissolved in 40 ml of water and added to the freshly prepared AgCl. The slurry was stirred and a sample was taken periodically for analysis by UV–visible spectroscopy. After ca. 4 h, the absorption at 430 nm had disappeared. The mixture was filtered and the filtrate was evaporated to dryness. The yellow residue was extracted with methanol and evaporated to dryness. Yield 1.3 g of yellow powder. IR (cm^{-1}): 1400 (b, m), 1230 (s), 1020 (w), 803 (w), 570 (w). ^{1}H NMR (D_2O): δ 3.08 ppm (s, $^2J_{Pt-H}$ 78 Hz). ^{13}C NMR (D_2O): 3.67 ppm (q, $^1J_{C-H}$ 145 Hz, $^1J_{C-Pt}$ 462 Hz). ^{195}Pt NMR (D_2O): −780 ppm. Anal. Calc. for $PtKCl_4(CH_3)(H_2O) \cdot (KCl)_{3.7}$: Pt, 29.38; K, 27.68; Cl, 41.11; C 1.8. Found: Pt, 29.38; K, 27.64; Cl, 38.38; C, 1.65%.

4.7. Synthesis of [$NMe_4]_2[PtCl_5(CH_3)$] (5)

$K_xCl_yPt(CH_3)$ (200 mg) was dissolved in 4 ml of water and loaded on an ion-exchange column charged with NMe_4^+ ions as described above. A yellow band, following an orange band, was collected after elution with water. The solution was evaporated to dryness under vacuum, leaving an orange solid. The solid was repeatedly washed with ethanol to remove excess NMe_4Cl. The residue was dissolved in methanol (30 ml) and filtered. Approximately 2 ml of a saturated solution of NMe_4Cl in methanol was added and the resulting pale-orange precipitate collected on a filter. Yield 34 mg. IR (KBr, cm^{-1}): 3448 (b,m), 3021 (vs), 2927 (m), 1488 (vs), 1460 (w), 1420 (w), 1291 (s), 1215 (m), 953 (s). Uv–visible (water, 25°C): λ_{max} = 364 nm, ε_{mol} = 142 (4) l mol^{-1} cm^{-1}; λ_{max} = 462 nm, ε_{mol} = 25 (2) l mol^{-1} cm^{-1}. Anal. Calc. for $PtCl_5(CH_3)(N(CH_3)_4)_2$: C, 20.18; H, 5.08; N, 5.23. Found: C, 20.03; H, 4.82; N, 4.99%.

4.8. Synthesis of $K_xCl_yPt(CH_2CH_2OH)$

K_2PtCl_4 (3.42 g, 8.24 mmol) was dissolved in 20 ml of water and 2-iodoethanol (430 ml, 5.5 mmol) was added. After ca. 0.5 h the solution darkened and a dark precipitate was formed. The mixture was allowed to stand overnight and then filtered. The red filtrate was evaporated to dryness under vacuum and the residue was extracted with methanol (2 × 25 ml). From the residue 2.24 g (5.4 mmol) of K_2PtCl_4 was re-isolated. The yellow methanol fraction was evaporated to dryness, yielding a yellow powder whose NMR spectrum (in D_2O) indicated the $[PtCH_2CH_2OH]$ moiety. The powder was dissolved in 20 ml of water and added to freshly precipitated AgCl. The slurry was stirred for 2 h, filtered and the filtrate evaporated to dryness, yielding 332 mg of yellow powder. The compound was stored at −60°C. IR (KBr, cm^{-1}): 3450 (b), 2978 (w), 2929 (m), 1414 (s), 1384 (s), 1242 (m), 1167 (m), 1071 (m), 968 (w), 917 (s), 825 (w), 788 (w), 550 (w, b).

4.9. Synthesis of $(NMe_4)Pt(CH_2CH_2OH)Cl_4$ and $(NMe_4)_2Pt(CH_2CH_2OH)Cl_5$ (6)

$K_xCl_yPtCH_2CH_2OH$ (300 mg) was dissolved in ca. 5 ml of water and loaded on to an ion-exchange column charged with NMe_4^+ ions as described above. A yellow band was collected (20 ml) after elution with deionized water. The solution was concentrated to ca. 3 ml. During this process, a yellow precipitate (yield 111 mg) was formed, which was collected on a filter. Its ^1H NMR spectrum (D_2O) corresponds to that reported previously [11]. The elemental analysis agrees best with a salt of a monoanion. Calc. for $PtCl_4(CH_2CH_2OH)(N(CH_3)_4)$: C, 15.80; H, 3.76; N, 3.07. Found: C, 16.30; H, 3.79; N, 3.65%. ^{195}Pt NMR (D_2O): −731 ppm ($[Pt(CH_2CH_2OH)Cl_4(H_2O)]^-$), −750 ppm ($[Pt(CH_2CH_2OH)Cl_5^{2-}]$). IR (KBr, cm^{-1}): 3048 (m), 3575 (b,s), 3020 (m), 2937 (m), 1482 (vs), 1439 (w), 1403 (w), 1384 (s), 1261 (w), 1170 (s), 1071 (s), 990 (m), 950 (vs), 913 (vs), 797 (m), 654 (w), 473 (w).

The yellow precipitate was dissolved in methanol. Addition of a saturated solution of NMe_4Cl in methanol followed by ethanol gave an orange powder, which was collected on a frit and dried in high vacuum. Its elemental analysis corresponds to the expected stoichiometry, $(NMe_4)_2Pt(CH_2CH_2OH)Cl_5$). Calc. for $PtCl_5(CH_2CH_2OH)(N(CH_3)_4)_2$: C, 21.23; H, 5.17; N, 4.95. Found: C, 20.90; H, 4.99; N, 5.07%. UV–Vis (water, 25°C): λ_{max} = 364 nm, ε_{mol} = 150 (5) l mol^{-1} cm^{-1}; λ_{max} = 468 nm, ε_{mol} = 20 (3) l mol^{-1} cm^{-1}.

4.10. Kinetics of nucleophilic displacement reactions

Solutions of the specified concentrations in Pt complex and Cl^- in H_2O were placed in 1 cm glass cuvets in the thermostated cuvet holder of the spectrophotometer. Spectra were recorded at preset intervals in the wavelength region between 250 and 500 nm, using the HP 89531A software package. In all cases isosbestic points were observed at ca. 395, 440 and 490 nm. The degree of reaction was monitored by following the absorption peak around 365 nm. Kinetic studies were also carried out by NMR, using approximately 0.01 M solutions of **6**. NMR tubes were placed in a 45°C water-bath and spectra were recorded periodically after cooling to ambient temperature; NMe_4^+ served as internal standard. The overall rates agreed with those determined by UV–visible spectroscopy, while accurate relative rates of nucleophilic attack by water vs. chloride were calculated from the relative amounts of glycol and chloroethanol formed at various chloride concentations.

Reactions of $PtMeCl_5^{2-}$ with other nucleophiles were similarly followed by NMR, with signals for $MeNO_2$ and $MeOPO_3^{3-}$ identified by comparison with authentic samples.

4.11. Kinetics of oxidation of Zeise's salt by $[PtCl_6]^{2-}$

Oxidations were carried out at constant ionic strength with various amounts NaCl and $NaClO_4$ as electrolytes. For these studies, Zeise's salt (obtained from Aldrich) and NaCl were used as received; $NaClO_4$ was extensively dried at 120°C under high vacuum; $Na_2PtCl_6 \cdot 6H_2O$ was dissolved in D_2O, filtered, evaporated to dryness and dried under vacuum until constant in weight (the color becomes bright yellow, in contrast to the orange salt, that contains water of crystallization). DCl solutions were prepared by dilution of a 37% stock solution (Cambridge Isotope Laboratories).

UV–visible spectrophotometry is unsuitable for this study, as the spectra of the substrate and oxidizing agent are not sufficiently different. Instead, ^1H NMR spectroscopy was used. Progress of the reaction was followed by monitoring the disappearance of signals due to the starting material **7** and the appearance of those for products **6** (at lower temperatures) or chloroethanol plus glycol (at high temperature). Data were analyzed as discussed in the main text.

4.12. Synthesis of ICH_2CD_2OH

Following previous reports on the synthesis of ICH_2CH_2OH from $ClCH_2COOH$ via $ClCH_2CH_2OH$ [26], chloroacetic acid (1.35 g, 14.3 mmol) was placed in a 100 ml three-necked flask. The flask was immersed in an ice-bath and allowed to cool to 0°C. $BD_3 \cdot THF$ (50 ml, 0.38 mol) in THF solution was slowly added over a period of 15 min. The reaction mixture was stirred at 0°C for 30 min and then at 25°C for 2 h. Excess borane was destroyed by adding 15 ml of water–THF (1 : 1) to the reaction mixture. The aqueous

phase was saturated with potassium carbonate, the THF layer was separated and the aqueous phase extracted with 4 × 20 ml of diethylether. The combined organic extracts were dried over magnesium sulfate. Evaporation of the solvent gave 1.16 g of $ClCH_2CD_2OH$ as a clear liquid, which was dissolved in 5 ml of dry acetone and added over 1 h to a refluxing solution of 2.1 g of NaI in 4 ml of dry acetone. The mixture was allowed to reflux for 19 h and then cooled to room temperature. Sodium chloride was filtered off and washed with 2 × 2 ml of acetone. Sodium iodide (0.12 g) was added to the filtrate and the mixture heated at reflux for 9 h, cooled and filtered to remove sodium chloride. Acetone was evaporated; the residue was extracted with 20 ml of diethylether, filtered and washed with 3 × 5 ml of diethylether. Evaporation of the ether gave 1.65 g (67%) of ICH_2CD_2OH. ^1H NMR ($CDCl_3$): δ 3.29 (s, 2H, ICH_2CD_2OH), δ 2.00 (s, 1H, ICH_2CD_2OH). The proton content at the $-C(H,D)_2OH$ position was about 3%.

4.13. Reduction of $[NMe_4]_2[PtMeCl_5]$ by $CrCl_2$ and $SnCl_2$

The dry reagents, $[NMe_4]_2[PtMeCl_5]$ (50 mg, 0.093 mmol) and $CrCl_2$ (25 mg, 0.20 mmol) or $SnCl_2$ (18 mg, 0.090 mmol), were combined and thoroughly mixed in a small flask equipped with a stirrer bar. The flask was placed on a high-vacuum line, evacuated and cooled to liquid nitrogen temperature. Degassed H_2O (5 ml) was condensed into the flask and allowed to warm. Upon thawing, the solution turned dark green (Cr^{II}) or orange–brown (Sn^{II}) and gas evolution was immediately apparent. The gas was collected and quantified using a Toepler pump and characterized as CH_4 by IR and ^1H NMR spectroscopy. Methane yield (based on **5**): 57% ($CrCl_2$) and 31% ($SnCl_2$).

4.14. Absence of exchange in $[PtCl_5CH_2CD_2OH]^{2-}$

$K_xCl_yPtCH_2CD_2OH$ was prepared from K_2PtCl_4 and ICH_2CD_2OH as described above for the undeuterated analog. The yield was 35%. The ^1H NMR spectrum (D_2O) showed only the signal (δ 3.85, $^2J_{PtH}$ = 85.0 Hz) assigned to the $-PtCH_2-$ position. A solution of 8.0 mg of $K_xCl_yPtCH_2CD_2OH$ and 87 mg of NaCl in 0.50 ml of D_2O was kept at 45°C for 8 h. The decomposition of $K_2Cl_5PtCH_2CD_2OH$ was essentially complete at this point. The ^1H NMR spectrum indicated that $ClCH_2CD_2OH$ was the only isotopomer of the organic product formed; no $HOCH_2CD_2Cl$ was detected.

4.15. Synthesis of $Na_2{}^{195}PtCl_6$ and $K_2{}^{195}PtCl_4$ from ^{195}Pt metal

^{195}Pt metal (97.3% ^{195}Pt) was purchased from Oak Ridge National Laboratory. $H_2{}^{195}PtCl_6$ was synthesized by the published procedure [27] and converted into $Na_2{}^{195}PtCl_6$ by ion exchange. $Na_2{}^{195}PtCl_4$ was prepared from $Na_2{}^{195}PtCl_6$ by the published procedure [28] and converted into $K_2{}^{195}PtCl_4$ by ion exchange.

4.16. Oxidation of Zeise's salt by $Na_2{}^{195}PtCl_6$

$KPtCl_3(CH_2{=}CH_2)\cdot H_2O$ (10 mg, 0.027 mmol) and $Na_2{}^{195}PtCl_6$ (27 mg, 0.060 mmol) were dissolved in 0.40 ml of D_2O (some $K_2{}^{195}PtCl_6$ precipitated immediately). After allowing the mixture to stand for 24 h at room temperature, ^1H NMR showed complete conversion to $[Cl_5PtCH_2CH_2OH]^{2-}$. The signal for the $[Cl_5PtCH_2CH_2OH]^{2-}$ protons exhibited ^{195}Pt satellites of normal intensity (ca. 33% of total peak area). If the solution was allowed to stand at room temperature for several days, the intensity of the satellites of $[Cl_5PtCH_2CH_2OH]^{2-}$ gradually increased.

4.17. Alkyl transfer between $[PtRCl_5]^{2-}$ and $[^{195}PtCl_4]^{2-}$

$(NMe_4)_2PtCl_5(CH_2CH_2OH)$ (7.0 mg, 0.012 mmol) and $K_2{}^{195}PtCl_4$ (5.1 mg, 0.012 mmol) were dissolved in 0.40 ml of D_2O. The ^1H NMR spectrum recorded after a few minutes showed satellites of the $PtCH_2CH_2OH$ signal with normal intensity (ca. 33% of total peak area). The solution was allowed to stand at room temperature and the extent of exchange was followed by monitoring the intensity of the satellites. After 2 days, their intensity had increased to 39% and after 14 days to 52%. A solution of $K_2PtCl_5CH_2CH_2OH$ and $Na_2{}^{195}PtCl_6$, handled similarly, showed *no* increase in the satellite peaks. Data were analyzed according to the rate law in the Appendix to determine the rate constant for alkyl exchange between Pt^{IV} and Pt^{II}.

Alkyl transfer between $[PtMeCl_5]^{2-}$ and $[^{195}PtCl_4]^{2-}$ was studied in the same manner, using a solution of $(NMe_4)_2PtMeCl_5$ (5.9 mg, 0.011 mmol) and $K_2{}^{195}PtCl_4$ (4.6 mg, 0.011 mmol) in 0.40 ml of D_2O at 1 M ionic strength ($NaClO_4$) (a small amount of white NMe_4ClO_4 precipitate formed). The total intensity of the $[PtCH_3Cl_5]^{2-}$ signal did not change relative to the HOD or NMe_4^+ signals during the kinetic experiment.

4.18. Stereochemical studies

cis- and *trans*-1,2-dideuterioethylene were purchased from Cambridge Isotope Laboratories. The corresponding stereolabeled Zeise's salts were prepared by the published procedure for ordinary Zeise's salt [29]. A solution of $K[PtCl_3(cis\text{- or }trans\text{-}1,2\text{-}C_2H_2D_2)]$ (70 mg) and $Na_2PtCl_6\cdot 6H_2O$ (1 g) in 20 ml of water was heated for 3 h at 45°C. After cooling and concentration to a few ml, KCl (260 mg) was added to precipitate excess $PtCl_6^{2-}$ as K_2PtCl_6, which was filtered off. An

aliquot of the filtrate was evaporated to dryness and its proton NMR spectrum was recorded in D_2O (see discussion in main text). The remaining solution was thermolyzed for 6 h at 45°C and vacuum transferred on to 3 ml of 12 M NaOH at liquid nitrogen temperature. Slow warming to room temperature resulted in a vigorous evolution of gas, which was collected by a Toepler pump (0.057 mmol, 30%) and vacuum transferred to a 10 cm IR gas cell (total pressure ca. 10 cm Hg). Analysis of the IR spectra as previously discussed [22] gave the stereochemistry and isotopomeric purity of the dideuterioethylene oxide.

Acknowledgments

This was supported by the Office of Naval Research and by Texaco. S.S.S. thanks the National Science Foundation for a predoctoral fellowship.

Appendix: Derivation of rate laws

Nucleophilic attack on alkylPt^{IV}

We have

$$\mathbf{5a} \overset{K_1}{\rightleftharpoons} \mathbf{5b} + Cl^- \overset{K_2}{\rightleftharpoons} \mathbf{5c} + Cl^-$$

where **5a**, **5b** and **5c** are as defined in Eq. (3) of the main text.

Disappearance of the starting complex, as monitored by UV–visible spectroscopy, follows:

$$d[Pt_{total}]/dt = -k_{obs}[Pt_{total}]$$

In case 1, **[5b]** is negligible, and products are formed from **5c** according to

$$\mathbf{5c} + Cl^- \xrightarrow{k_1} RCl + Pt^{II}$$

$$\mathbf{5c} + H_2O \xrightarrow{k_2} ROH + Pt^{II}$$

$$d[Pt_{total}]/dt = -(k_1[Cl^-] + k_2)[\mathbf{5c}]$$

$$[\mathbf{5c}][Cl^-]/[\mathbf{5a}] = K_1K_2$$

$$[\mathbf{5a}] = [\mathbf{5c}][Cl^-]/K_1K_2$$

$$[Pt_{total}] = [\mathbf{5a}] + [\mathbf{5c}] = [\mathbf{5c}]([Cl^-]/K_1K_2 + 1)$$

$$d[Pt_{total}]/dt = -\frac{(k_1[Cl^-] + k_2)[Pt_{total}]}{[Cl^-]/K_1K_2 + 1}$$

$$k_{obs} = \frac{k_1[Cl^-] + k_2}{[Cl^-]/K_1K_2 + 1}$$

In case 2, products are formed from **5b** according to

$$\mathbf{5b} + Cl^- \xrightarrow{k_1} RCl + Pt^{II}$$

$$\mathbf{5b} + H_2O \xrightarrow{k_2} ROH + Pt^{II}$$

$$d[Pt_{total}]/dt = -(k_1[Cl^-] + k_2)[\mathbf{5b}]$$

$$[\mathbf{5b}][Cl^-]/[\mathbf{5a}] = K_1$$

$$[\mathbf{5a}] = [\mathbf{5b}][Cl^-]/K_1$$

$$[\mathbf{5c}]/[\mathbf{5b}] = K_2$$

$$[\mathbf{5c}] = K_2[\mathbf{5b}]$$

$$[Pt_{total}] = [\mathbf{5a}] + [\mathbf{5c}] + [\mathbf{5b}]$$

$$= [\mathbf{5b}]([Cl^-]/K_1 + K_2 + 1)$$

$$d[Pt_{total}]/dt = -\frac{(k_1[Cl^-] + k_2)[Pt_{total}]}{[Cl^-]/K_1 + K_2 + 1}$$

$$k_{obs} = \frac{k_1[Cl^-] + k_2}{[Cl^-]/K_1 + K_2 + 1}$$

However, **[5b]** is very small, then $K_2 \gg 1$, so

$$k_{obs} \approx \frac{k_1[Cl^-] + k_2}{[Cl^-]/K_1 + K_2}$$

$$= \frac{(k_1[Cl^-] + k_2)/K_2}{[Cl^-]/K_1K_2 + 1}$$

which has the same form as that derived for case 1: the apparent equilibrium constant extracted from kinetic data will be equal to K_1K_2, the macroscopic constant relating **[5a]** and **[5b]**, in either case, while the apparent individual rate constants will be either the actual rate constants or $1/K_2$ times those values for cases 1 and 2, respectively.

Oxidation of Zeise's salt by $[PtCl_6]^{2-}$

Substituting $[H^+] = [7] - [7]_0$ into Eq. (17) gives

$$-d[7]/dt = kK[7][PtCl_6^{2-}]/([7] - [7]_0)$$

Rearranging:

$$-(d[7]/dt)([7] - [7]_0)/[7] = kK[PtCl_6^{2-}]$$

$$-[7]_0(d[7]/[7]) + d[7] = kK[PtCl_6^{2-}]\,dt$$

Integrating:

$$-[7]_0 \ln([7]/[7]_0) + [7] - [7]_0 = kK[PtCl_6^{2-}]t$$

which rearranges to Eq. (18).

References and notes

[1] J.A. Labinger, A.M. Herring and J.E. Bercaw, *J. Am. Chem. Soc.*, *112* (1990) 5628.

[2] J.A. Labinger, A.M. Herring, D.K. Lyon, G.A. Luinstra, J.E. Bercaw, I. Horváth and K. Eller, *Organometallics*, *12* (1993) 895.

[3] A. Sen, M. Lin, L.-C. Kao and A.C. Hutson, *J. Am. Chem. Soc.*, *114* (1992) 6385; A. Sen, M.A. Benvenuto, M.R. Lin, A.C.

Hutson and N. Basickes, *J. Am. Chem. Soc.*, *116* (1994) 998, and references cited therein.
[4] R.A. Periana, D.J. Taube, E.R. Evitt, D.G. Löffler, P.R. Wentrcek, G. Voss and T. Masuda, *Science*, *259* (1993) 340.
[5] W.E. Broderick, K. Kanamori, R.D. Willett and J.I. Legg, *Inorg. Chem.*, *30* (1991) 3875.
[6] Recently Zamashchikov et al. have offered an argument in support of the oxidative addition mechanism (V.V. Zamashchikov, V.G. Popov, E.S. Rudakov and S.A. Mitchenko, *Dokl. Akad. Nauk*, *333* (1993) 34); however, it depends on the assumption that formation of an alkane complex would have no isotope effect. In the light of the known isotope effects in agostic systems, their conclusions appear open to question.
[7] G.A. Luinstra, J.A. Labinger and J.E. Bercaw, *J. Am. Chem. Soc.*, *115* (1993) 3004.
[8] G.A. Luinstra, L. Wang, S.S. Stahl, J.A. Labinger and J.E. Bercaw, *Organometallics*, *13* (1994) 755.
[9] Proposed intermediate **2** ($R=CH_3$) was reported to have been detected by ^1H NMR in a cooled reaction mixture following oxidation of methane (K.A. Kushch, V.V. Lavrushko, Yu.S. Misharin, A.P. Moravsky, and A.E. Shilov, *New J. Chem.*, *7* (1983) 729); however, no corresponding signal was observed under reaction conditions using a high-pressure NMR cell: I.T. Horváth, R.A. Cook, J.M. Millar and G. Kiss, *Organometallics*, *12* (1993) 8.
10] (a) V.V. Zamashchikov, A.N. Kitaigorodskii, S.L. Litvinenko, E.S. Rudakov, O.N. Uzhik and A.E. Shilov, *Izv. Akad. Nauk. SSSR, Ser. Khim 8* (1985) 1730. (b) V.V. Zamashchikov, S.L. Litvinenko, and V.I. Shologon, *Kinet. Katal.*, *28* (1987) 1059, and references cited therein.
11] J. Halpern and R.A. Jewsbury, *J. Organomet. Chem.*, *181* (1979) 223.
12] (a) V.V. Zamashchikov, S.A. Mitchenko, E.S. Rudakov and T.M. Pekhtereva, *Koord. Khim.*, *11* (1985) 69; (b) V.V. Zamashchikov and S.A. Mitchenko, *Kinet. Katal.*, *24* (1983) 254.
13] J.P. Collman, L.S. Hegedus, J.R. Norton and R.G. Finke, *Principles and Applications of Organotransition Metal Chemistry*, University Science Books, Mill Valley, CA, 1987, p. 306.
[14] K.I. Goldberg, J. Yan and E.L. Winter, *J. Am. Chem. Soc.*, *116* (1994) 1573. The results do not exclude a six-coordinate solvated species, $[PtMe_3(dppe)(acetone)]^+$, as the key reactive intermediate; that would be the analog of **5c** in our system.
[15] A.C. Hutson and A. Sen, *Abstr. 204th National ACS Meeting, August 1992*, INOR-69.
[16] C.G. Swain and C.B. Scott, *J. Am. Chem. Soc.*, *75* (1953) 141.
[17] L. Melander and W.H. Saunders, *Reaction Rates of Isotopic Molecules*, Robert E. Krieger, Malabar, FL, 1987, pp. 173–174.
[18] These observations tend to suggest a predominantly inner-sphere electron transfer process (as perhaps also do the effects of buffers). The most common mechanism for oxidations by $[PtCl_6]^{2-}$ and related species is an inner-sphere, two-electron process, essentially a "chloronium ion" transfer, although a positive dependence on $[Cl^-]$ is usually observed in such cases (W.R. Mason, *Coord. Chem. Rev.*, *7* (1972) 241), in contrast to our findings. The detailed mechanism is yet to be established.
[19] A.C. Hutson, M. Lin and A. Sen, *Abstr. 206th National ACS Meeting, August 1993*, INOR-14.
[20] V.V. Zamashchikov, V.G. Popov and S.L. Litvinenko, *Russ. Chem. Bull.*, *42* (1993) 352.
[21] J.-E. Bäckvall, *Acc. Chem. Res.*, 16 (1983) 335, and references cited therein.
[22] L.L. Whinnery, Jr., L.M. Henling and J.E. Bercaw, *J. Am. Chem. Soc.*, *113* (1991) 7575.
[23] Yu.V. Geletii and A.E. Shilov, *Kinet. Katal.*, *24* (1983) 413.
[24] M.S. Freund, J.A. Labinger, N.S. Lewis and J.E. Bercaw, *J. Mol. Catal.*, *87* (1994) L11.
[25] T.G. Appleton, J.R. Hall and M.A. Williams, *J. Organomet. Chem.*, *303* (1986) 139.
[26] H.C. Brown, N.M. Yoon, C.S. Pak, S. Krishnamurthy and T.P. Stocky, *J. Org. Chem.*, *38* (1973) 2786; H. Wieland and E. Sakellarios, *Chem. Ber.*, *53* (1920) 208.
[27] D.C. Giedt and C.J. Nyman, *Inorg. Synth.*, *8* (1966) 239
[28] G.B. Kauffman and D.O. Cowan, *Inorg. Synth.*, *7* (1963) 240.
[29] P.B. Chock, J. Halpern and F.E. Paulik, *Inorg. Synth.*, *14* (1973) 90.